# IDENTIFICATION OF TRANSPORT PARAMETERS FOR GALLIUM NITRIDE BASED SEMICONDUCTOR DEVICES

V. Palankovski and A. Marchlewski, AMADEA Group, IuE, TU Vienna, Austria
E. Ungersböck and S. Selberherr, Inst. for Microelectronics, TU Vienna, Austria

Corresponding author: V. Palankovski
TU Vienna, Gusshausstr. 27-29/E360, A-1040 Vienna, Austria
Phone: +43 1 58801-36017, Fax: +43 1 58801-36099
email: palankovski@iue.tuwien.ac.at

**Abstract.** We present a methodology for the identification of transport parameters for Gallium Nitride (GaN) based semiconductor materials and devices. A Monte Carlo (MC) approach has been employed to investigate the electron transport in GaN and AlGaN, materials that are very important in device applications of high-power, high-frequency electronics. Our model is validated against measured data and compared to published simulation results. It enables to understand effects taking place in this material system, and it provides inputs for macroscopic modeling of electronic devices. Various MC model parameters and simulation results are compared. A special approach on the piezoelectric scattering mechanism taking care of the hexagonal crystal structure is used.

## 1. Motivation

Material models which incorporate the basic characteristics of the underlying physics in a given semiconductor material are the core of device modeling. While for Silicon such models are well established, models for GaN and GaN-related materials are a hot topic of present research activities. This material system recently became of interest for applications in optical, high-power, and high-frequency electronics. However, GaN still poses many technological as well as modeling challenges. Progress in assessing the entire material information is impeded experimentally by varying material quality and theoretically by the lack of detailed knowledge of relevant parameters. Examples are deformation potentials, piezo-parameters, etc.

## 2. Considerations on the Monte Carlo Approach

The MC method is a powerful technique to establish a consistent link between theory and experiments. It helps to gain understanding of the transport properties and it provides macroscopic parameters which are necessary for the description of electronic devices. We employ a single-particle MC technique to investigate stationary electron transport in GaN. Our model includes the three lowest valleys of the conduction band ($\Gamma_1$, U, $\Gamma_3$). Several stochastic mechanisms such as acoustic phonon, polar optical phonon, inter-valley phonon, ionized impurity scattering, and piezoelectric scattering are considered and their impact is assessed. The particular advantage of the MC method is that it provides a transport formulation on microscopic level, limited only by the extent to which the underlying physics of the system is included. Since the GaN material system is yet not so well explored, several important input parameters are still missing or just inaccurately known. We assess in an iterative approach the influence of the input parameters and their interdependencies in order to get a set of parameters which gives agreement with experimental data available for different physical conditions (doping, temperature, field, etc.). Such a calibrated set of models and model parameters delivers valuable data for low-field mobility, velocity saturation, energy relaxation times, etc. These calibrated models can serve as a basis for the development of analytical models for the simulation of GaN-based electron devices.

An accurate and often sufficient approximation for the conduction band is the parabolic approximation of the three lowest valleys. For values of the wave-vector far from the minima of the conduction band the energy deviates from the simple quadratic expression, and non-parabolicity occurs. The non-parabolic relationship between energy $\epsilon$ and wave vector $k$ is given by: $\gamma(\epsilon(k)) = \epsilon\,(1 + \alpha\,\epsilon) = \hbar^2 k^2/2\,m$, with $\alpha$ being the non-parabolicity factor and $m$ the effective electron mass.

In order to establish a rigorous MC simulation, parameters from various publications have been collected and analyzed. Table 1 and Table 2 provide a detailed summary of bulk material parameters for GaN and AlN, respectively, published throughout the past years. These tables include information necessary for analytical band-structure MC simulations, such as energies of lowest conduction bands, effective electron masses, non-parabolicity factors, and

**Table 1:** Summary of material parameters of wurtzite GaN for Monte Carlo simulation

| Bandgap energy | | | Electron mass | | | Non-parabolicity | | | Scattering models | | | | | | Reference |
|---|---|---|---|---|---|---|---|---|---|---|---|---|---|---|---|
| $\Gamma_1$ | U | $\Gamma_3$ | $m_{\Gamma 1}$ | $m_U$ | $m_{\Gamma 3}$ | $\alpha_{\Gamma 1}$ | $\alpha_U$ | $\alpha_{\Gamma 3}$ | ADP | $\hbar\omega_{ij}$ | $\hbar\omega_{LO}$ | $\rho$ | $\varepsilon_s$ | $\varepsilon_\infty$ | |
| [eV] | [eV] | [eV] | [$m_0$] | [$m_0$] | [$m_0$] | [1/eV] | [1/eV] | [1/eV] | [eV] | [meV] | [meV] | [g/cm$^3$] | [-] | [-] | Year |
| 3.5 | - | - | 0.19 | - | - | 0.187 | - | - | 12.0 | - | 99.5 | 6.1 | 9.5 | 5.35 | [1] 1975 |
| 3.5 | 5.00 | - | 0.19 | 1.00 | - | 0.187 | - | - | 12.0 | - | 92.0 | 6.1 | 9.5 | 5.35 | [2] 1993 |
| 3.5 | 5.00 | - | 0.19 | 0.7 | - | 0.187 | - | - | 12.0 | - | 92.0 | 6.1 | 9.5 | 5.35 | [3] 1995 |
| 3.4 | 5.50 | 5.60 | 0.19 | 0.41 | 0.41 | - | - | - | 10.1 | - | 92.0 | 6.095 | 9.5 | 5.35 | [4] 1995 |
| 3.5 | 5.50 | 5.60 | 0.20 | 0.40 | 0.60 | 0.183 | 0.065 | 0.029 | 8.3 | 92.9 | 92.9 | 6.1 | 8.9 | 5.35 | [5] 1997 |
| 3.39 | 5.39 | 5.59 | 0.20 | 0.40 | 0.60 | 0.189 | 0.067 | 0.029 | 8.3 | 91.2 | 91.2 | 6.15 | 8.9 | 5.35 | [6] 1998 |
| 3.5 | 4.99 | 5.25 | 0.20 | 0.24 | 0.40 | 0.19 | 0.17 | 0 | 7.8 | 65.0 | 92.0 | 6.095 | 9.5 | 5.35 | [7] 1998 |
| 3.5 | 5.40 | 5.60 | 0.20 | 1.00 | 1.00 | 0.189 | 0 | 0 | 8.3 | 91.2 | 91.2 | 6.15 | 8.9 | 5.35 | [8] 1999 |
| 3.5 | 5.50 | 5.60 | 0.19 | 0.40 | 0.60 | 0.183 | 0.065 | 0.029 | 10.1 | 92.0 | 92.0 | 6.1 | 8.9 | 5.35 | [9] 1999 |
| 3.5 | 5.45 | 5.60 | 0.21 | 0.25 | 0.40 | 0.19 | 0.1 | 0 | 8.0 | 65.0 | 92.0 | 6.095 | 9.5 | 5.35 | [10] 2000 |
| 3.36 | - | - | 0.20 | - | - | - | - | - | 10.1 | - | 92.0 | 6.095 | 9.5 | 5.35 | [11] 2000 |
| 3.52 | 5.77 | 5.87 | 0.212 | - | - | 0.37 | - | - | 8.3 | 65.8 | 90.88 | 6.087 | 9.7 | 5.28 | [12] 2001 |
| 3.5 | 4.5 | 4.6 | 0.186 | 0.40 | 0.60 | 0.189 | 0.065 | 0.029 | 8.3 | - | 99.5 | 6.15 | 9.5 | 5.35 | [13] 2002 |
| 3.52 | 5.77 | 5.87 | 0.212 | 0.493 | 0.412 | - | - | - | 8.3 | - | 90.88 | 6.087 | 9.7 | 5.28 | [14] 2002 |
| 3.5 | 5.60 | 3.90 | 0.20 | 0.60 | 0.22 | 0.183 | 0.029 | 0.065 | 8.3 | 80.0 | 26&92.2 | 6.15 | 9.95 | 5.35 | [15] 2004 |
| 3.39 | 5.29 | 5.59 | 0.20 | 1.00 | 1.00 | 0.189 | 0 | 0 | 8.3 | 92.0 | 92.0 | 6.15 | 8.9 | 5.35 | [16] 2005 |
| 3.39 | 5.29 | 5.49 | 0.20 | 0.30 | 0.40 | 0.189 | 0 | 0 | 8.3 | 91.0 | 92.0 | 6.1 | 8.9 | 5.35 | This work |

**Table 2:** Summary of material parameters of wurtzite AlN for Monte Carlo simulation.

| Bandgap energy | | | Electron mass | | | Non-parabolicity | | | Scattering models | | | | | | Reference |
|---|---|---|---|---|---|---|---|---|---|---|---|---|---|---|---|
| $\Gamma_1$ | U | $\Gamma_3$ | $m_{\Gamma 1}$ | $m_U$ | $m_{\Gamma 3}$ | $\alpha_{\Gamma 1}$ | $\alpha_U$ | $\alpha_{\Gamma 3}$ | ADP | $\hbar\omega_{ij}$ | $\hbar\omega_{LO}$ | $\rho$ | $\varepsilon_s$ | $\varepsilon_\infty$ | |
| [eV] | [eV] | [eV] | [$m_0$] | [$m_0$] | [$m_0$] | [1/eV] | [1/eV] | [1/eV] | [eV] | [meV] | [meV] | [g/cm$^2$] | [-] | [-] | Year |
| 6.20 | 6.90 | - | 0.48 | 1.0 | - | 0.044 | 0 | - | 9.5 | 99.2 | 99.2 | 3.23 | 8.5 | 4.77 | [17] 1998 |
| 5.84 | 7.00 | 8.29 | 0.326 | 0.384 | 0.473 | 0.29 | - | - | 9.5 | 75.8 | 110.3 | 3.23 | 8.5 | 4.46 | [12] 2001 |
| 6.00 | 7.05 | 8.49 | 0.26 | 0.495 | 0.55 | 0.207 | 0.035 | 0.023 | - | 76.1 | 110.7 | - | - | 4.68 | [18] 2002 |
| 6.20 | 6.90 | 8.20 | 0.33 | 0.40 | 0.50 | 0.044 | 0 | 0 | 9.5 | 99.2 | 99.2 | 3.23 | 8.5 | 4.77 | This work |

model parameters for the acoustic deformation potential (ADP) scattering, inter-valley scattering ($\hbar\omega_{ij}$), and polar optical phonon scattering ($\hbar\omega_{LO}$). $\varepsilon_\infty$ and $\varepsilon_s$ are the optical and static dielectric constants, $\rho$ is the mass density.

Our choice on the bandgap energies for GaN is based on one of the recent publications [16]. The particular setup for the masses has negligible impact within the available range, thus an average value similar to [10] has been chosen. Further parameters have been considered accordingly.

A complete set of material parameters for AlN is needed to model AlGaN, which is relevant for high-frequency amplifiers. We found only few publications which provide such parameter sets. For the simulation of AlGaN, an alloy scattering potential of 0.91 eV [18] is assumed. All other parameters are linearly interpolated between GaN and AlN.

## 3. Piezo-Scattering

An interesting result of the literature search performed for this work was the fact that in almost all MC simulations the piezo-scattering mechanisms were modeled assuming a cubic crystal structure. This is a correct approach to most of the technologically significant semiconductors, whereas for wurtzites the hexagonal structure has to be accounted for in the relevant piezo-scattering model.

In nitride crystals with wurtzite structure, elastic strain may be accompanied by macroscopic electric fields. This piezoelectric effect provides an additional coupling between the electron and acoustic vibrations [19].

The role of piezoelectric interaction in bulk wurtzite GaN has been recently analyzed by Kokolakis et al. [20]. In particular, the effect of acoustic piezoelectric scattering is taken in consideration, and the scattering rates have been calculated including the effect of screening. In accordance with their simulations, our results show that the piezo-acoustic rates are higher in the wurtzite phase than in the cubic phase, and they are very sensitive to the background doping of the sample. Since nitrides exhibit the largest piezoelectric constants among all of the III-V semiconductors an accurate modeling of piezoelectric scattering is especially important. In this work we present a piezoelectric scattering model similar to [19, 20], assuming equipartition, valid at temperatures over one Kelvin, considering non-parabolicity and screening in terms of the Thomas-Fermi inverse length $q_0$.

According to the Fermi Golden rule the probability rate for scattering from a state $\mathbf{k}$ to state $\mathbf{k}'$ is:

$$W(\mathbf{k} \to \mathbf{k}') = W_a + W_e = \frac{2\pi}{\hbar}|F(\mathbf{q})|^2 \left[n_{\mathbf{q}}\delta\left(\epsilon\left(\mathbf{k}+\mathbf{q}\right) - \epsilon\left(\mathbf{k}\right) - \hbar\omega_{\mathbf{q}}\right) + (n_q+1)\delta\left(\epsilon\left(\mathbf{k}-\mathbf{q}\right) - \epsilon\left(\mathbf{k}\right) - \hbar\omega_{\mathbf{q}}\right)\right]$$

where $W_a$ corresponds to absorption ($\mathbf{k}' = \mathbf{k}+\mathbf{q}$) and $W_e$ to emission ($\mathbf{k}' = \mathbf{k}-\mathbf{q}$) of a phonon with wave vector $\mathbf{q}$. The averaged coupling constant is obtained as:

$$|F(q)|^2 = C_0 K_{av} f(q); \qquad f(q) = \frac{q^3}{(q^2+q_0^2)^2}$$

The dimensionless constant $K_{av}$ is used to introduce the mean sound velocity $v_s$ which determines the energy of the averaged acoustic phonons $\hbar\omega_q = \hbar v_s q$. Employing the equipartition approximation $n_q = kT/\hbar\omega_q = kT/\hbar v_s q$, we obtain the scattering rates for emission and absorption.

$$\begin{aligned}
\lambda_e &= \mathrm{C}_1(\epsilon(k)) \int_0^{x_3} \frac{x^3}{(x^2+1)^2} dx - \mathrm{C}_2(\epsilon(k)) \int_0^{x_3} \frac{x^4}{(x^2+1)^2} dx \\
\lambda_a &= \mathrm{C}_1(\epsilon(k)) \int_{x_1}^{x_2} \frac{x^3}{(x^2+1)^2} dx + \mathrm{C}_2(\epsilon(k)) \int_{x_1}^{x_2} \frac{x^4}{(x^2+1)^2} dx
\end{aligned}$$

where $x = q/q_0$ is the normalized wave vector, and $\mathrm{C}_1$, $\mathrm{C}_2$ are sound velocity dependant coupling constants, proportional to $K_{av}$.

Almost all the works listed in Table 1 used a piezo-scattering model valid only for cubic crystals. In such a model the electromechanical coupling coefficient $K_{av,C}$ can be calculated by (1) with the piezo-coefficient $e_{14}$ and the longitudinal and transverse elastic constants $c_\mathrm{L}$ and $c_\mathrm{T}$ [19]. The latter can be obtained from (2) and (3), respectively, from the electromechanical coupling coefficients $c_{11}$, $c_{12}$, and $c_{44}$ or from the longitudinal and transverse sound velocities $v_\mathrm{sl}$ and $v_\mathrm{st}$, if known.

$$K^2_{\mathrm{av,C}} = e^2_{14} \cdot (12/c_\mathrm{L} + 16/c_\mathrm{T}) \,/\, (35 \cdot \varepsilon_\mathrm{s}) \tag{1}$$

$$c_\mathrm{L} = 0.6 \cdot c_{11} + 0.4 \cdot c_{12} + 0.8 \cdot c_{44}; \qquad v_\mathrm{sl} = \sqrt{c_\mathrm{L}/\rho} \tag{2}$$

$$c_\mathrm{T} = 0.2 \cdot c_{11} - 0.2 \cdot c_{12} + 0.6 \cdot c_{44}; \qquad v_\mathrm{st} = \sqrt{c_\mathrm{T}/\rho} \tag{3}$$

**Table 3:** Summary of elastic constants of GaN and AlN and the resulting longitudinal and transverse elastic constants and sound velocities.

| $c_{11}$ | $c_{12}$ | $c_{44}$ | GaN | $c_\mathrm{L}$ | $c_\mathrm{T}$ | $v_\mathrm{sl}$ | $v_\mathrm{st}$ | $c_{11}$ | $c_{12}$ | $c_{44}$ | AlN | $c_\mathrm{L}$ | $c_\mathrm{T}$ | $v_\mathrm{sl}$ | $v_\mathrm{st}$ |
|---|---|---|---|---|---|---|---|---|---|---|---|---|---|---|---|
| [GPa] | [GPa] | [GPa] | Data Refs. | [GPa] | [GPa] | [m/s] | [m/s] | [GPa] | [GPa] | [GPa] | Data Refs. | [GPa] | [GPa] | [m/s] | [m/s] |
| 296 | 120 | 24 | exp. [21] | 245 | 50 | 6342 | 2855 | 345 | 125 | 118 | exp. [22] | 351 | 115 | 10430 | 5962 |
| 374 | 106 | 101 | exp. [23] | 348 | 114 | 7557 | 4331 | 411 | 149 | 125 | exp. [24] | 406 | 127 | 11214 | 6280 |
| 390 | 145 | 105 | exp. [25] | 376 | 112 | 7859 | 4290 | 410 | 140 | 120 | exp. [26] | 398 | 126 | 11100 | 6246 |
| 377 | 160 | 81 | exp. [27] | 355 | 92 | 7637 | 3888 | 380 | 114 | 109 | calc. [28] | 361 | 119 | 10569 | 6060 |
| 365 | 135 | 109 | exp. [29] | 360 | 111 | 7693 | 4278 | 464 | 149 | 128 | calc. [30] | 440 | 140 | 11677 | 6579 |
| 370 | 145 | 90 | exp. [26] | 364 | 108 | 7733 | 4212 | 424 | 103 | 138 | calc. [31] | 406 | 147 | 11211 | 6746 |
| 373 | 141 | 94 | exp. [32] | 355 | 103 | 7641 | 4110 | 398 | 140 | 96 | calc. [33] | 372 | 109 | 10726 | 5814 |
| 369 | 94 | 118 | calc. [31] | 353 | 126 | 7620 | 4546 | 396 | 137 | 116 | calc. [34] | 385 | 121 | 10920 | 6131 |
| 396 | 144 | 91 | calc. [33] | 368 | 105 | 7775 | 4153 | 398 | 142 | 127 | calc. [35] | 397 | 127 | 11089 | 6280 |
| 367 | 135 | 95 | calc. [34] | 350 | 103 | 7585 | 4122 | | | | | | | | |
| 350 | 140 | 101 | calc. [35] | 347 | 103 | 7548 | 4106 | | | | | | | | |

**Table 4:** Summary of piezo coefficients of GaN and AlN for Monte Carlo simulation of piezo scattering.

| $e_{15}$ | $e_{31}$ | $e_{33}$ | GaN | | $\langle e_{\mathrm{L}}^2 \rangle$ | $\langle e_{\mathrm{T}}^2 \rangle$ | $e_{15}$ | $e_{31}$ | $e_{33}$ | AlN | | $\langle e_{\mathrm{L}}^2 \rangle$ | $\langle e_{\mathrm{T}}^2 \rangle$ |
|---|---|---|---|---|---|---|---|---|---|---|---|---|---|
| [C/m$^2$] | [C/m$^2$] | [C/m$^2$] | Data | Refs. | [C$^2$/m$^4$] | [C$^2$/m$^4$] | [C/m$^2$] | [C/m$^2$] | [C/m$^2$] | Data | Refs. | [C$^2$/m$^4$] | [C$^2$/m$^4$] |
| -0.30 | -0.36 | 1.00 | exp. | [36] | 0.103 | 0.123 | -0.48 | -0.58 | 1.55 | exp. | [22] | 0.251 | 0.304 |
| - | -0.55 | 1.12 | exp. | [37] | 0.175 | 0.234 | - | -0.60 | 1.50 | exp. | [37] | 0.260 | 0.334 |
| - | -0.33 | 0.65 | calc. | [1] | 0.061 | 0.082 | -0.29 | -0.58 | 1.39 | exp. | [38] | 0.102 | 0.230 |
| - | -0.49 | 0.73 | calc. | [39] | 0.118 | 0.149 | - | -0.60 | 1.46 | calc. | [39] | 0.251 | 0.326 |
| -0.22 | -0.22 | 0.43 | calc. | [40] | 0.027 | 0.036 | - | -0.38 | 1.29 | calc. | [35] | 0.169 | 0.187 |
| - | -0.32 | 0.63 | calc. | [35] | 0.058 | 0.077 | - | -0.64 | 1.80 | calc. | [41] | 0.349 | 0.429 |
| - | -0.44 | 0.86 | calc. | [41] | 0.109 | 0.145 | | | | | | | |

Table 3 summarizes the experimental and theoretical values of the elastic constants $c_{11}$, $c_{12}$, and $c_{44}$, available for wurtzite GaN and AlN in the literature. From them we calculated the corresponding $c_{\mathrm{L}}$, $c_{\mathrm{T}}$, $v_{\mathrm{sl}}$, and $v_{\mathrm{st}}$. We adopted the latest experimental values for GaN [32] and AlN [26] in our MC simulation. Note, that there are also experimental and theoretical values of the elastic constants for cubic GaN and AlN, but these are not relevant for this work.

Table 4 summarizes the experimental and theoretical values of the piezo coefficients $e_{15}$, $e_{31}$, and $e_{33}$, available for GaN and AlN in the literature. In cases, where $e_{15}$ is not available $e_{15} = e_{31}$ is assumed. From them, we calculated the corresponding $\langle e_{\mathrm{L}}^2 \rangle$ and $\langle e_{\mathrm{T}}^2 \rangle$, which are necessary to obtain the coupling coefficient $K_{av,WZ}$ by (4) taking into account the wurtzite structure.

$$\begin{aligned} \langle e_{\mathrm{L}}^2 \rangle &= 1/7 \cdot e_{33}^2 + 4/35 \cdot e_{33} \left(e_{31} + 2 \cdot e_{15}\right) + 8/105 \cdot \left(e_{31} + 2 \cdot e_{15}\right)^2 \\ \langle e_{\mathrm{T}}^2 \rangle &= 2/35 \cdot \left(e_{33} - e_{31} - e_{15}\right)^2 + 16/105 \cdot \left(e_{33} - e_{31} - e_{15}\right) + 16/35 \cdot e_{15}^2 \\ K_{\mathrm{av,WZ}}^2 &= \left(\langle e_{\mathrm{L}}^2 \rangle / c_{\mathrm{L}} + \langle e_{\mathrm{T}}^2 \rangle / c_{\mathrm{T}}\right) / \varepsilon_{\mathrm{s}} \end{aligned} \tag{4}$$

In order to compare MC simulations which consider the piezo-scattering we took the extreme values of $c_{\mathrm{L}}$ and $c_{\mathrm{T}}$ from Table 3 and computed the value ranges for cubic $\mathrm{K}_{av,C}$ using (1). Only in the case of [14] where $c_{\mathrm{L}}$ and $c_{\mathrm{T}}$ are provided, $\mathrm{K}_{av}$ can be estimated exactly. The results are presented in Table 5, where it is getting obvious that most authors either underestimate or even neglect the piezo-scattering effect, or use a higher $e_{14}$ value in their MC simulations to arrive at hexagonal-like piezo-scattering rates using (1). On the other hand, most of the MC simulations assume relatively low sound velocity values which lead to an overestimation of the ADP scattering rate. This is another reason for many authors to find piezo-scattering to be negligible compared to ADP scattering, which we observe is not always the case.

**Table 5:** Parameter values for the piezo scattering model.

| Ref. | $v_{\mathrm{sl}}$ [m/s] | $v_{\mathrm{st}}$ [m/s] | $e_{14}$ [C/m$^2$] | $c_{\mathrm{L}}$ [GPa] | $c_{\mathrm{T}}$ [GPa] | $\mathrm{K}_{av}$ [-] |
|---|---|---|---|---|---|---|
| [1] | 5000 | - | 0.560 | 245-376 | 50-126 | 0.13 - 0.20 |
| [4] | 4330 | - | none | - | - | - |
| [5] | 6600 | 2700 | 0.375 | 245-376 | 50-126 | 0.09 - 0.13 |
| [6] | 6560 | 2680 | 0.375 | 245-376 | 50-126 | 0.09 - 0.13 |
| [7] | 4330 | - | 0.560 | 245-376 | 50-126 | 0.13 - 0.20 |
| [8] | 6560 | 2680 | 0.375 | 245-376 | 50-126 | 0.09 - 0.13 |
| [9] | 4330 | - | none | - | - | - |
| [10] | 4330 | - | none | - | - | - |
| [11] | 6560 | - | none | - | - | - |
| [12] | 7619 | - | 0.375 | 245-376 | 50-126 | 0.09 - 0.13 |
| [13] | 4330 | - | 0.375 | 245-376 | 50-126 | 0.09 - 0.13 |
| [14] | 7619 | - | 0.368 | 266 | 62 | 0.117 |
| [15] | 8000 | 4860 | 0.375 | 245-376 | 50-126 | 0.09 - 0.13 |
| [16] | 6560 | - | none | - | - | - |
| This work | 7641 | 4110 | - | 355 | 103 | 0.137 |

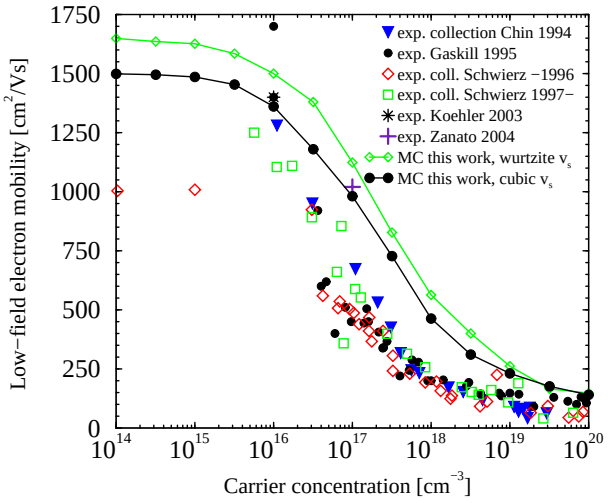


**Figure 1:** Low-field electron mobility as a function of carrier concentration in GaN. Comparison of the MC simulation results and experimental data.

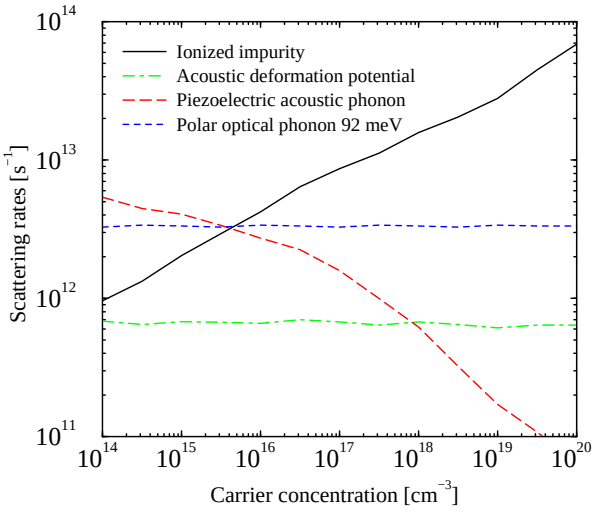


**Figure 2:** Illustration of the scattering rates in our simulation for wurtzite GaN as a function of doping concentration at 300 K.

## 4. Simulation Results

Using the established setup of models and model parameters, we obtained MC simulation results for different physical conditions (doping, temperature, field, etc.) for bulk GaN, AlN, and AlGaN. Fig. 1 shows the low-field electron mobility in hexagonal GaN as a function of free carrier concentration. Two MC simulation curves are included to demonstrate the effect of the difference between the cubic and hexagonal sound velocities and their impact on the low-field mobility. The mobility depends on the sound velocity via the piezo and the ADP scattering mechanism. A higher sound velocity reduces the ADP scattering rate, which results in an increased mobility as illustrated in Fig. 1.

Fig. 2 shows the corresponding scattering rates as a function of the doping concentration in hexagonal GaN. Note, that the piezoelectric scattering is the dominant mobility limitation factor at low concentrations even at room temperature, beside the commonly accepted importance at low temperatures.

Our MC simulation is in fairly good agreement with experimental data from collections or single point measurements from [42, 43, 44, 45, 46]. The electron mobilities, selected for comparisons in this work, consider bulk material and are measured using the Hall effect. The discrepancy between our simulation results and the measured data might be attributed to dislocation scattering which is not considered in our work. This mechanism is considered to be a source of mobility degradation for GaN samples.

Numerous publications on GaN heterostructure devices (see e.g. a summary in [47]) provide inversion layer mobilities which are higher. These values are derived from transit frequency and device dimensions. However, two-dimensional electron gas heterostructures are plagued, among others, by surface scattering effects, and are not considered in this work.

Fig. 3 shows the low-field electron mobility as a function of lattice temperature in GaN at $10^{17}$ cm$^{-3}$ concentration. The experimental data are from [46, 48, 49]. Note, that mobility increases over the years because of the improved material quality (reduced dislocation density).

Fig. 4 provides the electron drift velocity versus the electric field. We compare our MC result with other simulations [4, 5, 7, 12, 15, 50], and with the available experimental data [51, 52]. The low field data points are in qualitatively good agreement, at higher fields experimental values are significantly lower. Both experiments [51, 52] of electron velocities in bulk GaN, employ pulsed voltage sources. Many devices with etched constrictions were measured and the peak electron drift velocity $v_{\mathrm{d,max}}$ was typically found to be about $2.5\times10^7$ cm/s at electric fields $E_{\mathrm{pk}}$=180 kV/cm. An overview of characteristic MC simulation results of GaN is summarized in Table 6. The discrepancy in the MC results comes from differently chosen sets of parameter values and considerations of scattering mechanisms.

A recent publication of Brazis et al. [15] on MC simulation of GaN provided a good fit to experimental results. It introduces a satellite valley close to the bottom of the conduction band and additional low-energy optical phonon

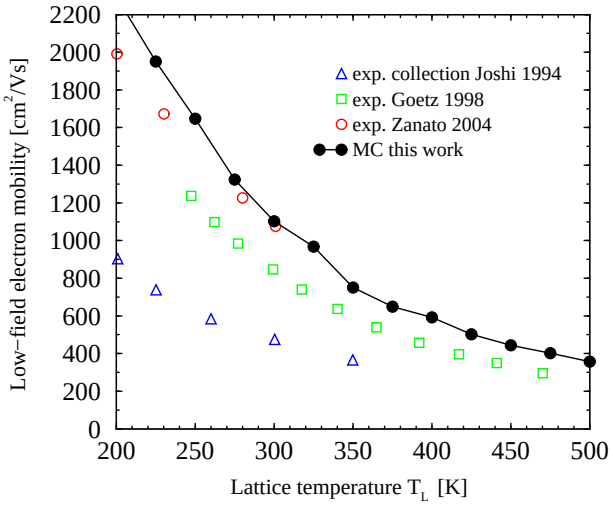


**Figure 3:** Low-field electron mobility as a function of lattice temperature in GaN at carrier concentration of $10^{17}$ cm$^{-3}$.

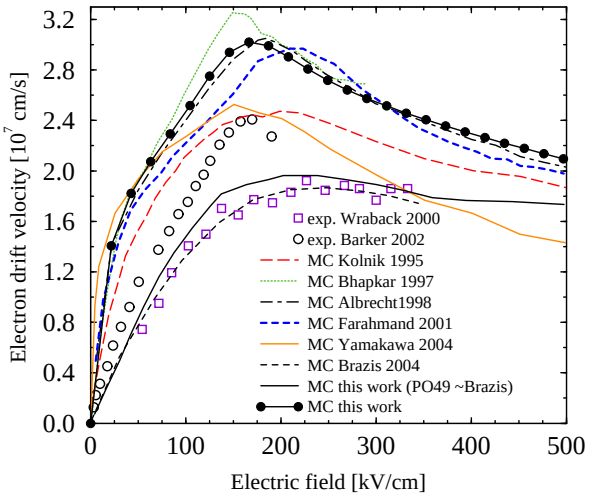


**Figure 4:** Drift velocity vs. electric field in wurztite GaN: Comparison of MC simulation results and experimental data.

**Table 6:** Comparison of drift velocity characteristic results of GaN MC.

| Reference | [1] | [2] | [3] | [4] | [5] | [6] | [7] | [8] | [9] | [10] | [11] | [12] | [13] | [14] | [15] | [16] | [50] | This work |
|---|---|---|---|---|---|---|---|---|---|---|---|---|---|---|---|---|---|---|
| $v_{\mathrm{d,max}}$ $10^5$[m/s] | 2.0 | 2.7 | 2.8 | 2.5 | 3.2 | 3.1 | 3.0 | 2.9 | 3.3 | 2.6 | 2.6 | 3.0 | 2.5 | 2.6 | 1.9 | 2.5 | 2.5 | 3.1 |
| $E_{\mathrm{pk}}$ [kV/cm] | 100 | 130 | 160 | 190 | 150 | 150 | 195 | 140 | 180 | 150 | 180 | 200 | 200 | 150 | 225 | 180 | 150 | 166 |
| $v_{\mathrm{sat}}$ $10^5$[m/s] | - | 1.5 | 1.6 | 1.9 | 2.5 | 2.5 | 2.1 | 1.4 | 1.5 | 1.8 | 2.0 | 1.9 | 1.7 | 2.4 | 1.8 | 1.3 | 1.4 | 2.1 |

modes of 26 meV. Using the MC parameter setup proposed by Brazis et al. and an averaged value for the polar optical phonon energy, between 92 meV and 26 meV, enabled us to arrive at a similar simulation result, validating the experimental result of [52] for a thin GaN film on a sapphire substrate.

Fig. 5 compares our MC simulation result for AlN against others from [12, 17, 53]. Our simulation results are in good agreement with [12, 17], since we use similar MC parameters as shown in Table 2. The difference visible at high fields can be explained by different effective electron masses used in the higher valleys. The simulation of [53] differs at low fields, since it ignores some mechanisms, e.g. ionized-impurity scattering.

Fig. 6 shows calculated electron steady-state drift velocity versus applied electric field in $Al_{0.2}Ga_{0.8}N$. Our choice for a mole fraction of 0.2 in the illustration is based on the observation that alloy compositions in a range between 0.15 and 0.3 promise high mobilities [11, 12] and thus, e.g., highest transit frequencies in amplifier devices. As can be seen from Fig. 6 our result is in good agreement with other MC simulation results [11, 12]. Although an exact comparison cannot be performed, experimental data of Barker et al. [54] from $Al_{0.2}Ga_{0.8}N$/GaN heterostructure are added.

## 5. Conclusion

Development of models for carrier transport in GaN-based materials gains importance. After careful review of available experimental and theoretical achievements, we developed a rigorous MC model, with the focal point on the piezo-scattering mechanisms in hexagonal crystal structures. It enables to understand the important effects taking place in this material system, and it allows creating analytical models for predictive device simulation.

## Acknowledgment

This work is supported by the Austrian Science Funds FWF, START Project No.Y247-N13. Special thanks go to Prof. Mihail Nedjalkov on his priceless help on understanding and implementation of the piezo-scattering mechanism and Dr. Rüdiger Quay for his inspiring correspondence and discussions.

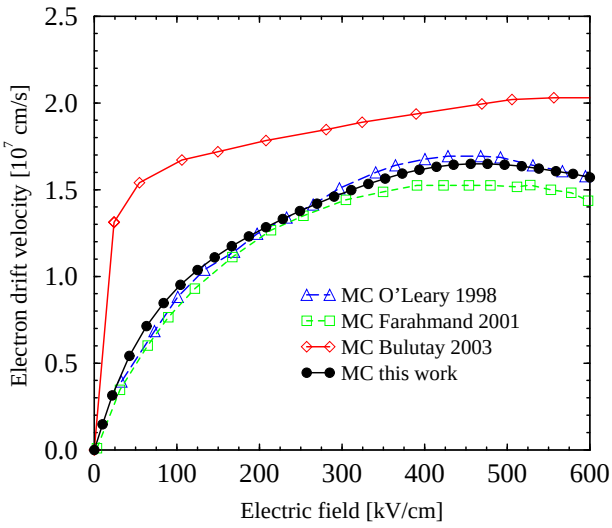


**Figure 5:** Drift velocity vs. electric field in wurtzite AlN: Comparison to other MC simulations.

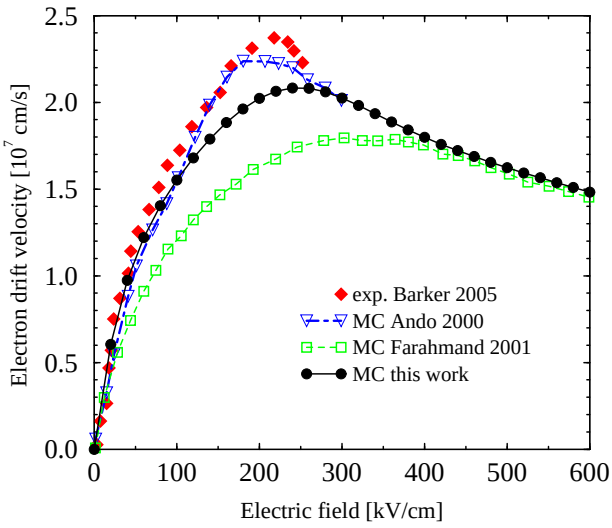


**Figure 6:** Drift velocity vs. electric field in wurtzite $Al_{0.2}Ga_{0.8}N$: Comparison to other MC simulations.

## References


[1] M. Littlejohn, J. Hauser, and T. Glisson, "Monte Carlo Calculation of the Velocity-Field Relationship for Gallium Nitride," *Appl.Phys.Lett.*, vol. 26, no. 11, pp. 625–627, 1975.

[2] B. Gelmont, K. Kim, and M. Shur, "Monte Carlo Simulation of Electron Transport in Gallium Nitride," *J.Appl.Phys.*, vol. 74, no. 3, pp. 1818–1821, 1993.

[3] N. Mansour, K. Kim, and M. Littlejohn, "Theoretical Study of Electron Transport in Gallium Nitride," *J.Appl.Phys.*, vol. 77, no. 6, pp. 2834–2836, 1995.

[4] J. Kolnik, I. Oguzman, K. Brennan, R. Wang, P. Ruden, and Y. Wang, "Electronic Transport Studies of Bulk Zincblende Wurtzite Phases of GaN Based on an Ensemble Monte Carlo Calculation Including a Full Zone Band Structure," *J.Appl.Phys.*, vol. 78, no. 2, pp. 1033–1038, 1995.

[5] U. Bhapkar and M. Shur, "Monte Carlo Calculation of Velocity-Field Characteristics of Wurtzite GaN," *J.Appl.Phys.*, vol. 82, no. 4, pp. 1649–1655, 1997.

[6] S. O'Leary, B. Foutz, M. Shur, U. Bhapkar, and L. Eastman, "Electron Transport in Wurtzite Indium Nitride," *J.Appl.Phys.*, vol. 83, no. 2, pp. 826–829, 1998.

[7] J. Albrecht, R. Wang, and P. Ruden, "Electron Transport Characteristics of GaN for High Temperature Device Modeling," *J.Appl.Phys.*, vol. 83, no. 9, pp. 4777–4781, 1998.

[8] B. Foutz, S. O'Leary, M. Shur, and L. Eastman, "Transient Electron Transport in Wurtzite GaN, InN, and AlN," *J.Appl.Phys.*, vol. 85, no. 11, pp. 7727–7734, 1999.

[9] J. Cao and X. Lei, "Nonparabolic Multivalley Balance-Equation Approach to Impact Ionization: Application to Wurtzite GaN," *The European Phys. Journal B*, vol. 7, pp. 79–83, 1999.

[10] T. Li, R. Joshi, and C. Fazi, "Monte Carlo Evaluations of Degeneracy and Interface Roughness Effects on Electron Transport in AlGaN-GaN Heterostructures," *J.Appl.Phys.*, vol. 88, no. 2, pp. 829–837, 2000.

[11] Y. Ando, W. Contrata, N. Samoto, H. Miyamoto, K. Matsunaga, M. Kuzuhara, K. Kunihiro, K. Kasahara, T. Nakayama, Y. Takahashi, N. Hayama, and Y. Ohno, "Gate Length Scaling for $Al_{0.2}Ga_{0.8}N$/GaN HJFETs: Two-Dimensional Full Band Monte Carlo Simulation Including Polarization Effect," *IEEE Trans.Electron Devices*, vol. 47, no. 10, pp. 1965–1972, 2000.

[12] M. Farahmand, C. Garetto, E. Bellotti, K. Brennan, M. Goano, E. Ghillino, G. Ghione, J. Albrecht, and P. Ruden, "Monte Carlo Simulation of Electron Transport in the III-Nitride Wurtzite Phase Materials System: Binaries and Ternaries," *IEEE Trans.Electron Devices*, vol. 48, no. 3, pp. 535–542, 2001.

[13] D. Herbert, M. Uren, B. Hughes, D. Hayes, J. Birbeck, R. Balmer, T. Martin, G. Crow, R. Abram, M.Walmsley, R. Davies, R. Wallis, W. Phillips, and S. Jones, "Monte Carlo Simulations of AlGaN/GaN Heterojunction Field-Effect Transistors (HFETs)," *J.Phys.:Condensed Matter*, vol. 14, no. 13, pp. 3479–3497, 2002.

[14] T.-H. Yu and K. Brennan, "Monte Carlo Calculation of Two-Dimensional Electron Dynamics in GaN-AlGaN Heterostructures," *J.Appl.Phys.*, vol. 91, no. 6, pp. 3730–3737, 2002.

[15] R. Brazis and R. Raguotis, "Additional Phonon Modes and Close Satellite Valleys Crucial for Electron Transport in Hexagonal Gallium Nitride," *J.Appl.Phys.*, vol. 85, no. 4, pp. 609–611, 2004.

[16] A. Reklaitis and L. Reggiani, "Monte Carlo Study of Hot-Carrier Transport in Bulk Wurtzite GaN and Modeling of a Near-Terahertz Impact Avalanche Transit Time Diode," *J.Appl.Phys.*, vol. 95, no. 2, pp. 7925–7935, 2004.

[17] S. O'Leary, B. Foutz, M. Shur, U. Bhapkar, and L. Eastman, "Monte Carlo Simulation of Electron Transport in Wurtzite Aluminum Nitride," *Solid-State Comm.*, vol. 105, no. 10, pp. 621–626, 1998.

[18] C. Bulutay, "Electron Initiated Impact Ionization in AlGaN Alloys," *Semicond.Sci.Technol.*, vol. 17, no. 10, pp. L59–L62, 2002.

[19] B. Ridley, *Quantum Processes in Semiconductors*. Oxford University Press, third ed., 1993.

[20] G. Kokolakis, J. Gleize, A. Cardo, and P. Lugli, "Exciton Interaction with Piezoelectric and Polar Optical Phonons in Bulk Wurtzite GaN," *Semicond.Sci.Technol.*, vol. 19, no. 4, pp. 460–462, 2004.

[21] V. Savastenko and A. Sheleg, "Study of the Elastic Properties of Gallium Nitride," *Phys.stat.sol.(a)*, vol. 48, no. 2, pp. 135–144, 1978.

[22] K. Tsubouchi and N. Mikoshiba, "Zero-Temperature-Coefficient SAW Devices on A1N Epitaxial Films," *IEEE Trans.Sonics Ultrason.*, vol. 32, no. 5, pp. 634–644, 1985.

[23] Y. Takagi, M. Ahart, T. Azuhata, T. Sota, K. Suzuki, and S. Nakamura, "Brillouin Scattering Study in the GaN Epitaxial Layer," *Physica B*, vol. 547, no. 9, pp. 219–220, 1996.

[24] L. McNeil, M. Grimsditch, and R. French, "Vibrational Spectroscopy of Aluminum Nitride," *J. American Cer. Soc.*, vol. 76, no. 5, pp. 1132–1138, 1993.

[25] A. Polian, M. Grimsditch, and I. Gregory, "Elastic Constants of Gallium Nitride," *J.Appl.Phys.*, vol. 79, no. 6, pp. 3343–3344, 1996.

[26] C. Deger, E. Born, H. Angerer, O. Ambacher, M. Stutzmann, J. Hornstein, E. Riha, and G. Fischerauer, "Sound Velocity of $Al_xGa_{1-x}N$ Thin Films Obtained by Surface Acoustic-Wave Measurements," *Appl.Phys.Lett.*, vol. 72, no. 19, pp. 2400–2402, 1998.

[27] R. Schwarz, K. Khachaturyan, and E. Weber, "Elastic Moduli of Gallium Nitride," *Appl.Phys.Lett.*, vol. 70, no. 9, pp. 1122–1124, 1997.

[28] R. Kato and J. Jama, "First-Principles Calculation of the Elastic Stiffness Tensor of Aluminium Nitride under High Pressure," *J.Phys.:Condensed Matter*, vol. 6, no. 38, pp. 7617–7632, 1994.

[29] M. Yamaguchi, T. Yagi, T. Azuhata, T. Sota, K. Suzuki, S. Chichinu, and S. Nakamura, "Brillouin Scattering Study of Gallium Nitride: Elastic Stiffness Constants," *J. Phys.: Condens.Matter*, vol. 9, no. 1, pp. 241–248, 1997.

[30] E. Ruiz, S. Alvarez, and P. Alemany, "Electronic Structure and Properties of AlN," *Phys.Rev.B*, vol. 49, no. 11, pp. 7115–7123, 1994.

[31] T. Azuhata, T. Sota, and K. Suzuki, "Elastic Constants of III-V Compound Semiconductors: Modification of Keyes' Relation," *J.Phys.:Condensed Matter*, vol. 8, no. 18, pp. 3111–3119, 1996.

[32] T. Deguchi, D. Ichiryu, K. Toshikawa, K. Sekiguchi, T. Sota, R. Matsuo, T. Azuhata, M. Yamaguchi, T. Yagi, S. Chichibu, and S. Nakamura, "Structural and Vibrational Properties of GaN," *J.Appl.Phys.*, vol. 86, no. 4, pp. 1860–1866, 1999.

[33] K. Kim, W. Lambrecht, and B. Segall, "Elastic Constants and Related Properties of Tetrahedrally Bonded BN, AlN, GaN, and InN," *Phys.Rev.B*, vol. 53, no. 24, pp. 16310–16326, 1996.

[34] A. Wright, "Elastic Properties of Zinc-Blende and Wurtzite AlN, GaN, and InN," *J.Appl.Phys.*, vol. 82, no. 6, pp. 2833–2839, 1997.

[35] K. Shimada, T. Sota, and K. Suzuki, "First-Principles Study on Electronic and Elastic Properties of BN, AIN and GaN," *J.Appl.Phys.*, vol. 84, no. 9, pp. 4951–4959, 1998.

[36] G. O'Clock and M. Duffy, "Acoustic Surface Wave Properties of Epitaxially Grown Aluminum Nitride and Gallium Nitride on Sapphire," *Appl.Phys.Lett.*, vol. 23, no. 2, pp. 55–56, 1973.

[37] I. Guy, S. Muensit, and E. Goldys, "Extensional Piezoelectric Coefficients of Gallium Nitride and Aluminium Nitride," *Appl.Phys.Lett.*, vol. 75, no. 26, pp. 4133–4136, 1999.

[38] G. Bu, D. Ciplys, M. Shur, L. Schowalter, S. Schujman, and R. Gaska, "Electromechanical Coupling Coefficient for Surface Acoustic Waves in Single-Crystal Bulk Aluminium Nitride," *Appl.Phys.Lett.*, vol. 84, no. 23, pp. 4611–4614, 2004.

[39] F. Bernardini and V. Fiorentini, "Spontaneous Polarization and Piezoelectric Constants of III-V Nitrides," *Phys.Rev.B*, vol. 56, no. 16, pp. R10024–R10027, 1997.

[40] A. Bykhovski, B. Gelmont, and M. Shur, "Elastic Strain Relaxation and Piezoeffect in GaN-AlN, GaN-AlGaN and GaN-InGaN Superlattices," *J.Appl.Phys.*, vol. 81, no. 9, pp. 6332–6338, 1997.

[41] A. Zoroddu, F. Bernardi, P. Ruggerone, and V. Fiorentini, "First-principles Prediction of Structure, Energetics, Formation Enthalpy, Elastic Constants, Polarization, and Piezoelectric Constants of AlN, GaN, and InN: Comparison of Local and Gradient-corrected Density-functional Theory," *Phys.Rev.B*, vol. 64, no. 4, p. 45208, 2001.

[42] F. Schwierz, "An Electron Mobility Model for Wurtzite GaN," *Solid-State Electron.*, vol. 49, no. 6, pp. 889–895, 2005.

[43] V. Chin, T. Tansley, and T. Osotachn, "Electron Mobilities in Gallium, Indium, and Aluminium Nitride," *J.Appl.Phys.*, vol. 75, no. 11, pp. 7365–7372, 1994.

[44] D. Gaskill, L. Rowland, and K. Doverspike, "Electrical Properties of AlN, GaN, and AlGaN," in *Properties of Group III Nitrides* (J. Edgar, ed.), no. 11 in EMIS Datareviews Series, section 3.2, pp. 101–116, IEE INSPEC, 1994.

[45] K. Köhler, S. Müller, N. Rollbühler, R. Kiefer, R. Quay, and G. Weimann, "Multiwafer Epitaxy of AlGaN/GaN Heterostructures for Power Applications," in *Proc. Intl. Symp. Compound Semiconductors* (M. Ilegems, ed.), (Lausanne), pp. 235–238, IOP Publishing, 2003.

[46] D. Zanato, N. Balkan, G. Hill, and W. J. Schaff, "Energy and Momentum Relaxation of Electrons in Bulk and 2D GaN," *Superlattices & Microstructures*, vol. 36, no. 4-6, pp. 455–463, 2004.

[47] M. Shur and R. Gaska, "Physics of GaN-based Heterostructure Field Effect Transistors," in *Comp.Semicond. IC Symp. Tech.Dig.*, pp. 137–140, 2005.

[48] R. Joshi, "Temperature-dependent Electron Mobility in GaN: Effects of Space Charge and Interface Roughness Scattering," *Appl.Phys.Lett.*, vol. 64, no. 2, pp. 223–225, 2004.

[49] W. Götz, N. Johnson, C. Chen, H. Liu, C. Kuo, and W. Ilmler, "Activation Energies of Si Donors in GaN," *Appl. Phys. Let.*, vol. 6, no. 22, pp. 3144–3147, 1996.

[50] S. Yamakawa, S. Aboud, M. Sarantini, and S. Goodnick, "Influence of Electron-Phonon Interaction on Electron Transport in Wurtzite GaN," *Semicond.Sci.Technol.*, vol. 19, no. 4, pp. 475–477, 2004.

[51] M. Wraback, H. Shen, J. Carrano, T. Li, J. Campbell, M.J.Schurman, and I. Ferguson, "Time-Resolved Electroabsorption Measurement of the Electron Velocity-Field Characteristic in GaN," *Appl. Phys. Let.*, vol. 76, no. 9, pp. 1154–1157, 2000.

[52] J. Barker, R. Akis, D. Ferry, S. Goodnick, T. Thornton, D. Kolesk, A. Wickenden, and R. Henry, "High-Field Transport Studies of GaN," *Physica B*, vol. 314, no. 1-4, pp. 39–41, 2002.

[53] C. Bulutay, B. Ridley, and N. Zakhleniuk, "Electron Momentum and Energy Relaxation Rates in GaN and AlN in the High-Field Transport Regime," *Phys.Rev.B*, vol. 68, no. 11, pp. 115205 1–7, 2003.

[54] J. Barker, D. Ferry, D. Koleske, and R. Shul, "Bulk GaN and AlGaN/GaN Heterostructure Drift Velocity Measurements and Comparison to Theoretical Models," *J.Appl.Phys.*, vol. 97, no. 6, 2005.